Supplementary Material

Probing Atomic-Scale Processes at the Ferrihydrite-Water Interface With Reactive Molecular Dynamics

Ardalan Hayatifar[1*], Simon Gravelle[2], Beatriz D. Moreno[3], Valerie A. Schoepfer[1], and Matthew B.J. Lindsay[1*]

[1]Department of Geological Sciences, University of Saskatchewan, Saskatoon, SK, Canada S7N 5E2
[2]University Grenoble Alpes, CNRS, LIPhy, 38000 Grenoble, France
[3]Science Division, Canadian Light Source, Saskatoon, SK, Canada

[*]Corresponding author: ardalan.hayatifar@usask.ca
[*]Corresponding author: matt.lindsay@usask.ca

DOI: 10.1186/s12932-024-00094-8

Contents

1 X-ray Reflectivity Measurements

X-ray reflectivity (XR) measurements were performed at Brockhouse Undulator Beamline (BXDS-IVU) at the Canadian Light Source (CLS). Specular XR measurements were conducted at a fixed energy (9.95 keV - $\lambda = 1.246$ Å), the reflectivity (i.e., the ratio of reflected to incident flux) of X-rays from the sample surface is measured versus 2θ, where 2θ is the angle between the incident and reflected beams, and λ is the wavelength of the X-ray beam). By varying the incident angle, a range of 2θ values from 0° to 2° is obtained.

The measurements were conducted in a flow cell made (Figure-1) in-house by Ted Toporowski at the Physics Shop at the University *of* Saskatchewan with the original designs generously shared by Dr. Sang Soo Lee. The flow cell was connected to a syringe pump and the sample was covered by Kapton® tape. XR are highly sensitive to sample crystallinity and surface roughness. The surface roughness also determines the resolution scale.

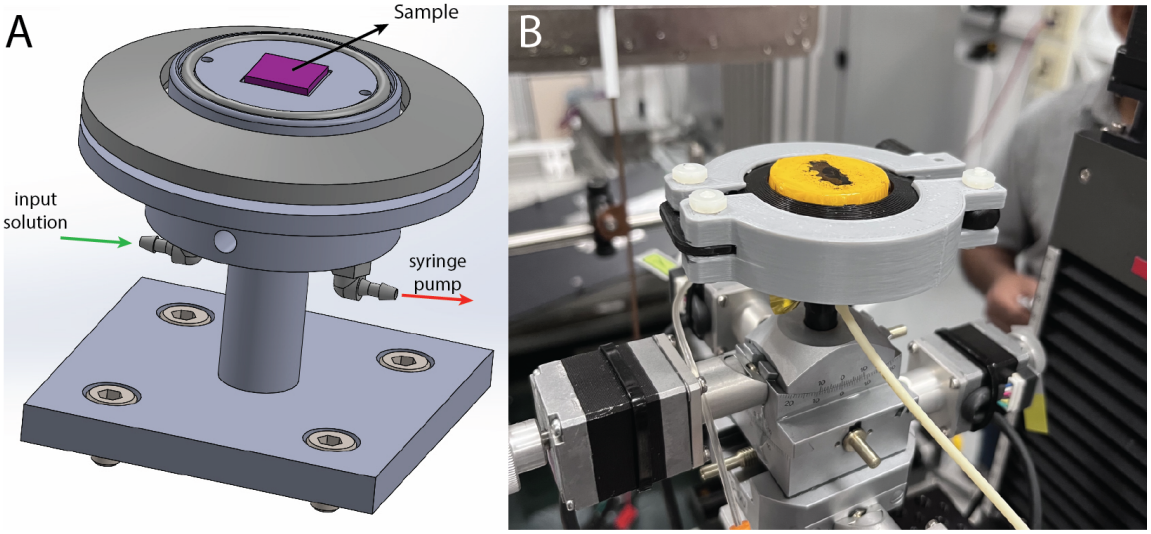

Figure 1: XR setup at the BXDS beamline. A) Prototype Design for the Flow Cell: this design showcases the sample position as well as the path through which the input solution enters and exits the cell. B) Final Setup at CLS-BXDS beamline: This image depicts the final setup featuring a Kapton window and Ferrihydrite powder at the BXDS beamline at the Canadian Light Source. (Input Solution: Displayed is the input solution being drawn using a syringe pump for precise fluid control.)

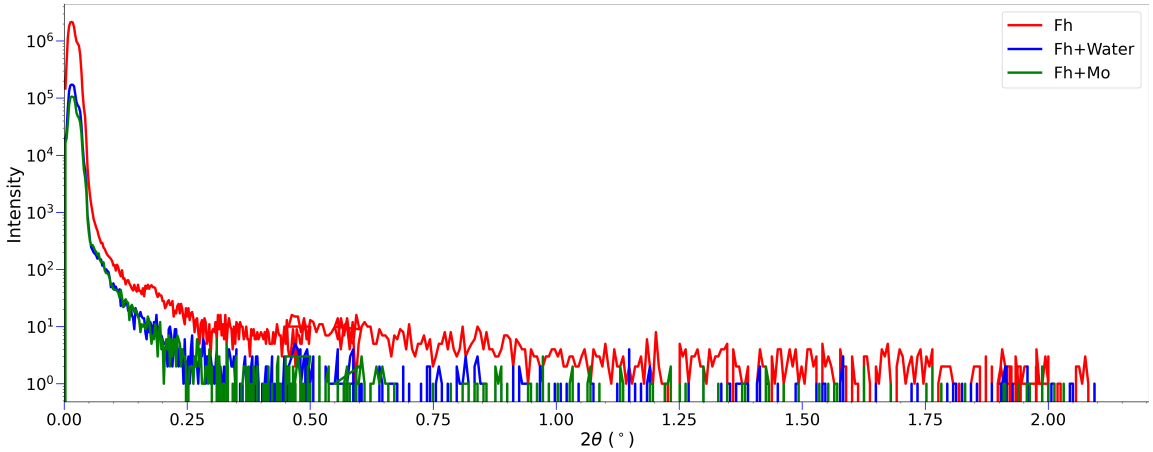

Figure 2: XR Experiments. XR measurements of Fh, Fh/water, and Fh/water/$MoO_{4(aq)}$

2 Radial Distribution Function Analysis of Ferrihydrite Structures

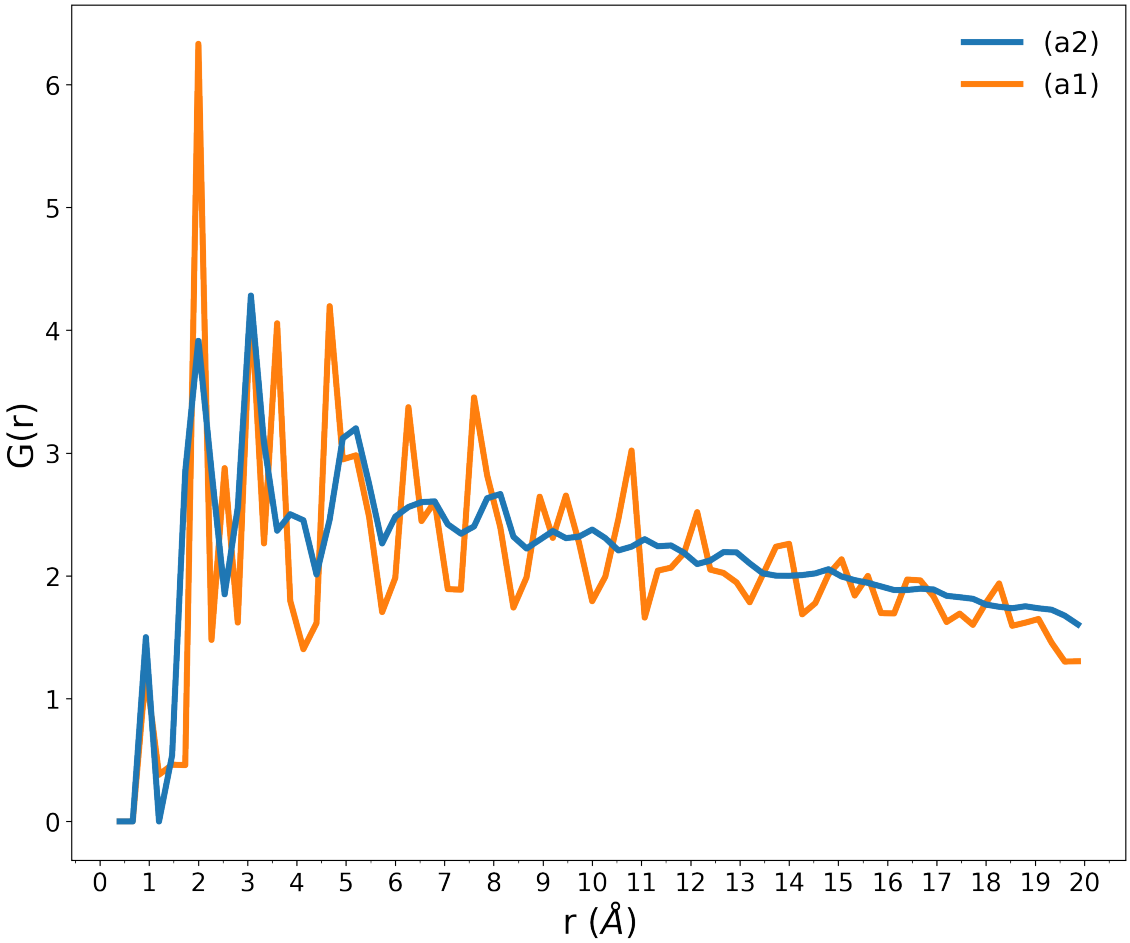

Figure 3: Calculated RDF analysis of Fh: effect of MD on the initial structure. Radial distribution function (RDF) from molecular dynamics (MD)- for Fh and the starting Michel model Fh. a1) Michel model, a2) relaxed slab of Fh

2.1 XRD: Phase Identification Results

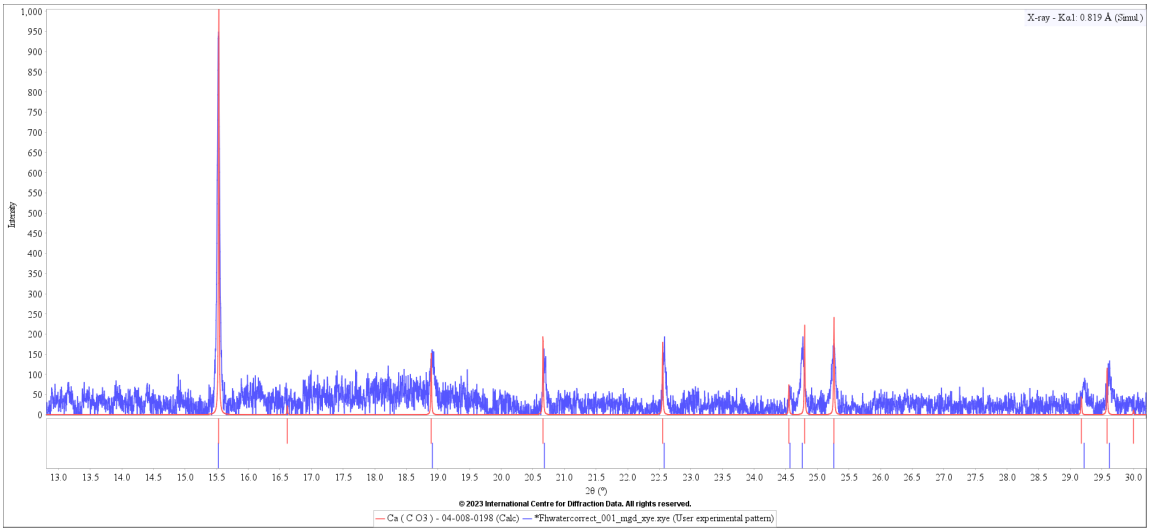

Figure 4: Phase analysis of the sharp features in the XRD pattern of Fh-water samples (Main text -Figure-?? (b2)) Background- subtracted XRD pattern of sharp features in Fh-water (b2) matched with calcite $CaCO_3$ structure (powder diffraction file # 04-008-0198) at λ=0.819 Å.

3 Pair Distribution Function Measurements

3.1 Differential Pair Distribution Function

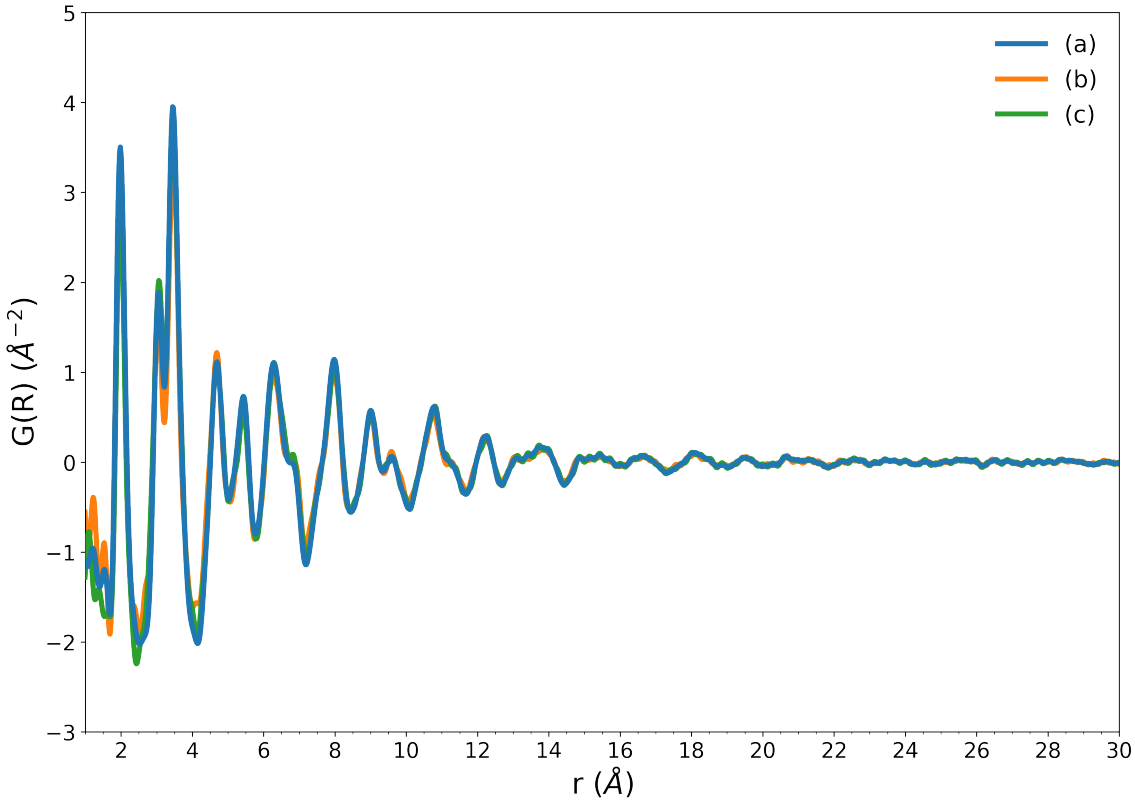

Figure 5: Experimental Pair distribution function (PDF) measurements. PDF of a) Fh, b) Fh-water mixture, and c) Fh-$[Mo]_{aq}$

4 Charge Analysis

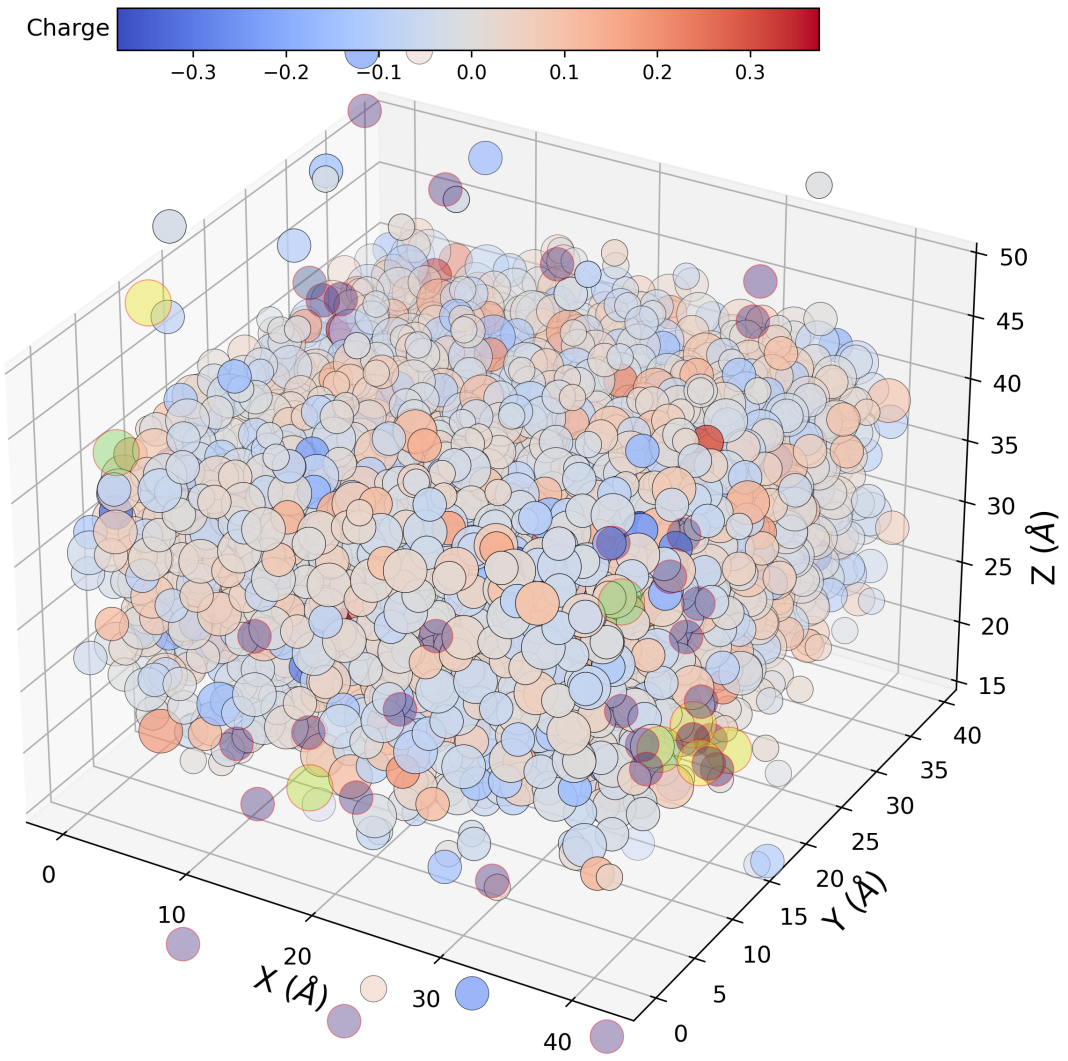

Figure 6: Charge analysis of ferrihydrite (Fh) with adsorbed $[Mo]_{aq}$. Calculated equilibrium atomic charge differences between Mo-0 and Mo-8 with explicitly shown $[Mo]_{aq}$ species. Note that species with red border colors belong to MoO_4^{2-} group, and species with black border color belong to Fh group. water and Na are not shown for clarity.

4.1 Charge Distribution Analysis

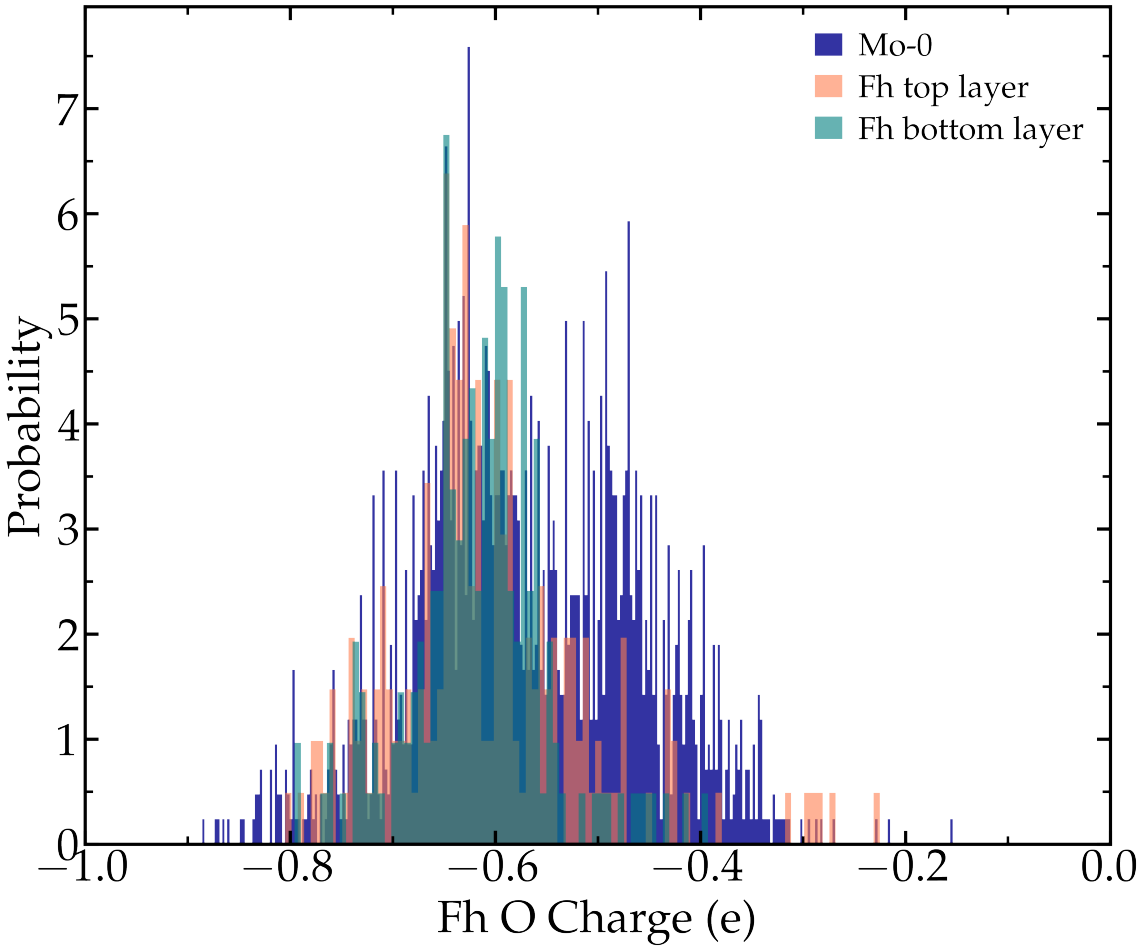

Figure 7: Charge Distribution in Fh and water. Charge probability distribution for Mo-0. Oxygen atoms consist of two main type: more negative interfacial oxygens and bulk oxygens. Identification of truly interfacial molecules (ITIM) analysis for both sides of the Fh slab (Fh top and bottom layers) indicates that the more negative oxygens belong to intefacial regions of Fh.

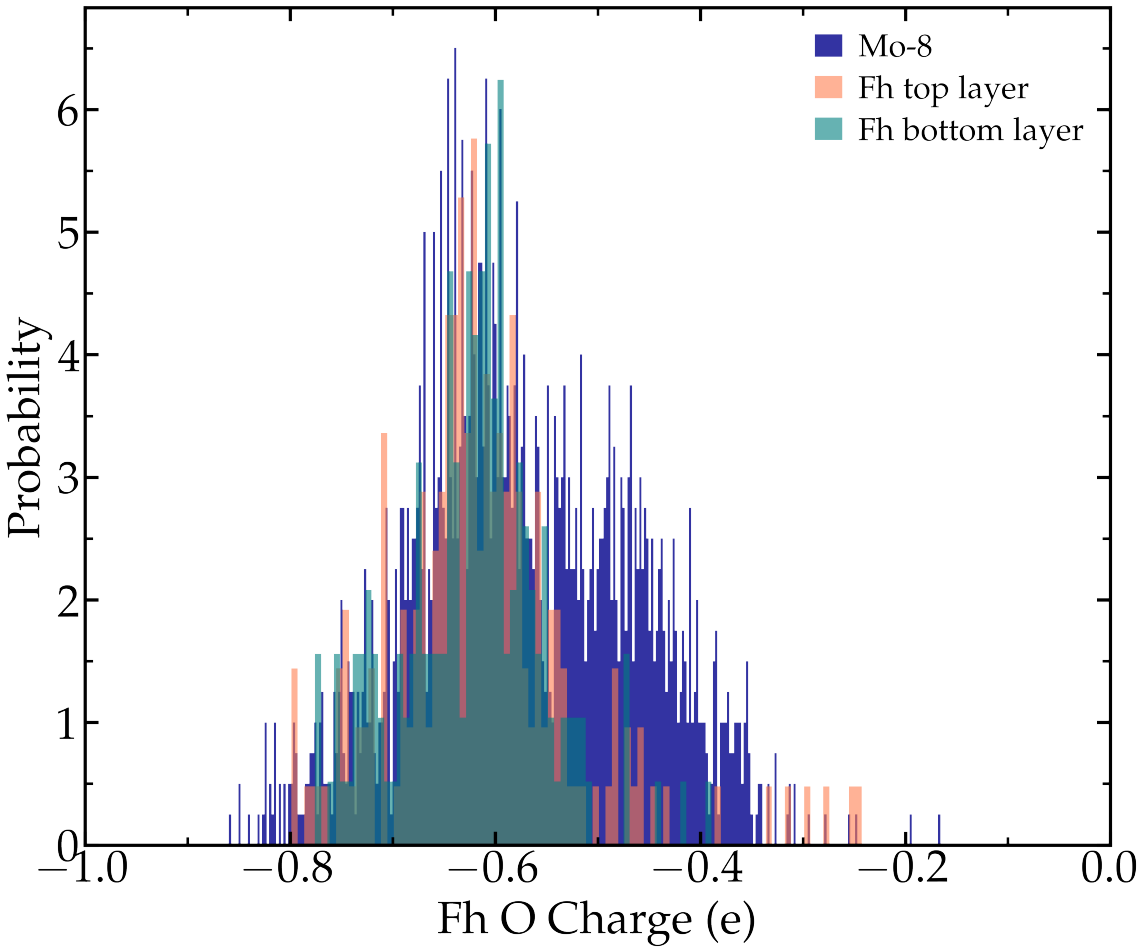

Figure 8: Charge Distribution in Fh and water with adsorbed $[Mo]_{aq}$. Charge probability distribution for Mo-8. ITIM analysis for both sides of the Fh slab (Fh top and bottom layers) indicates that the more negative oxygens belong to intefacial regions of Fh.

5 Fe-O-Fe Angle Distribution in Ferrihydrite

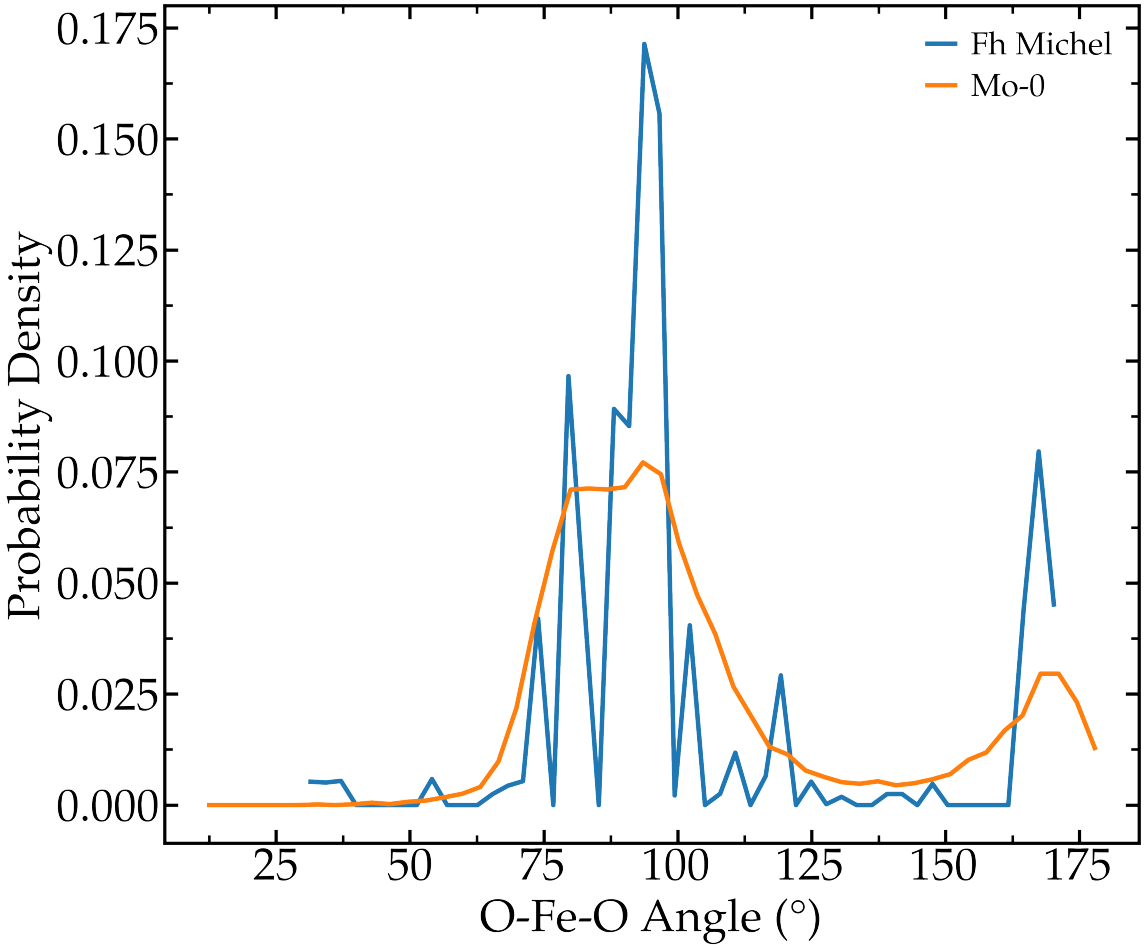

Figure 9: Fh Fe−O−Fe angle distribution in water. Probability distribution for Fe−O−Fe angle (°) for initial ideal Michel Fh and MD-relaxed Mo-0.

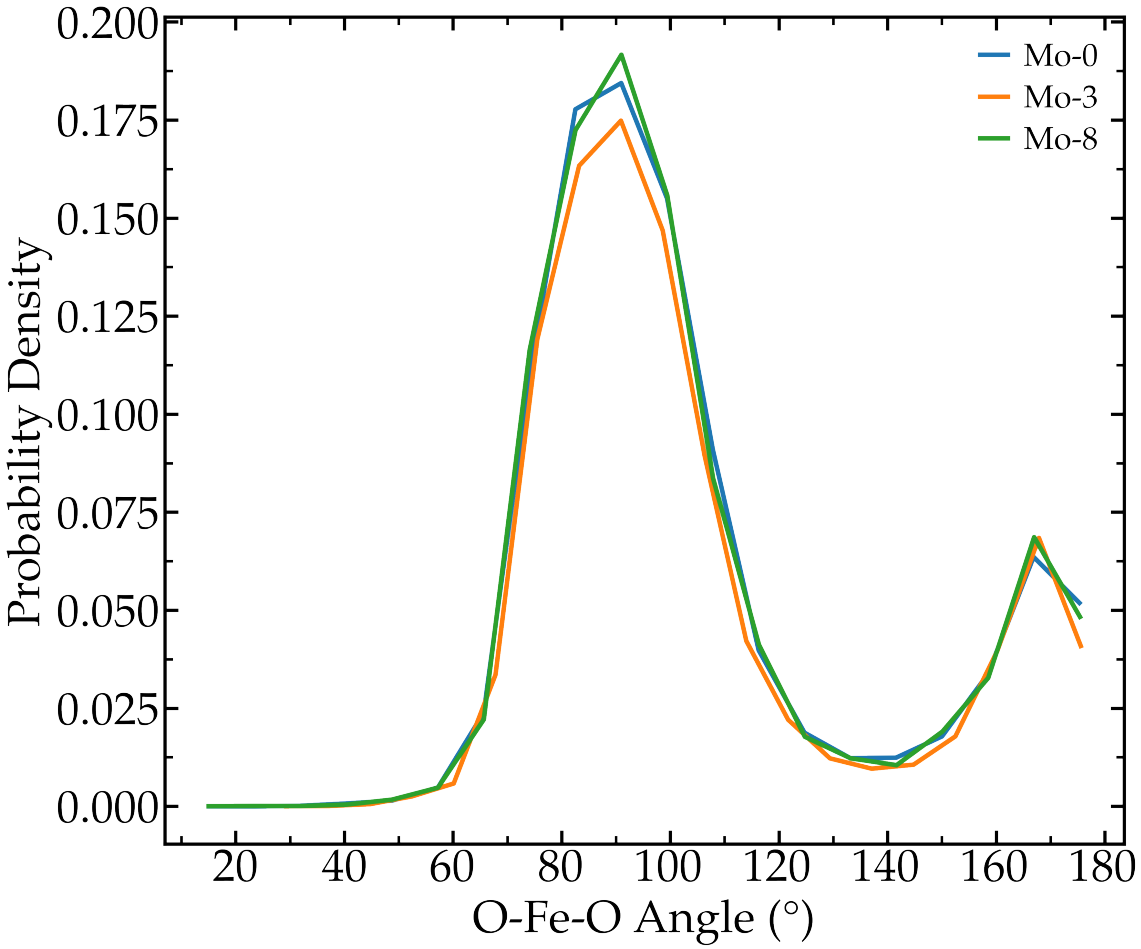

Figure 10: Fh Fe−O−Fe angle distribution in water and with adsorbed $[\mathbf{Mo}]_{\mathbf{aq}}$. Probability distribution for Fe−O−Fe angle (°) for Mo-0, 3, and 8.

6 Hydrogen Bond Analysis

For the scope of our analysis, a hydrogen bond (HB) is considered to be formed when the donor-acceptor distance - specified for different types of donors and acceptors such as O_f for Fh, O_m for Mo_{aq}, and O_w for water— is less than 3 Å, and the donor-hydrogen-acceptor angle is 30° or less.The analysis was performed using MDAnalysis Hydrogen Bond Analysis module [1].

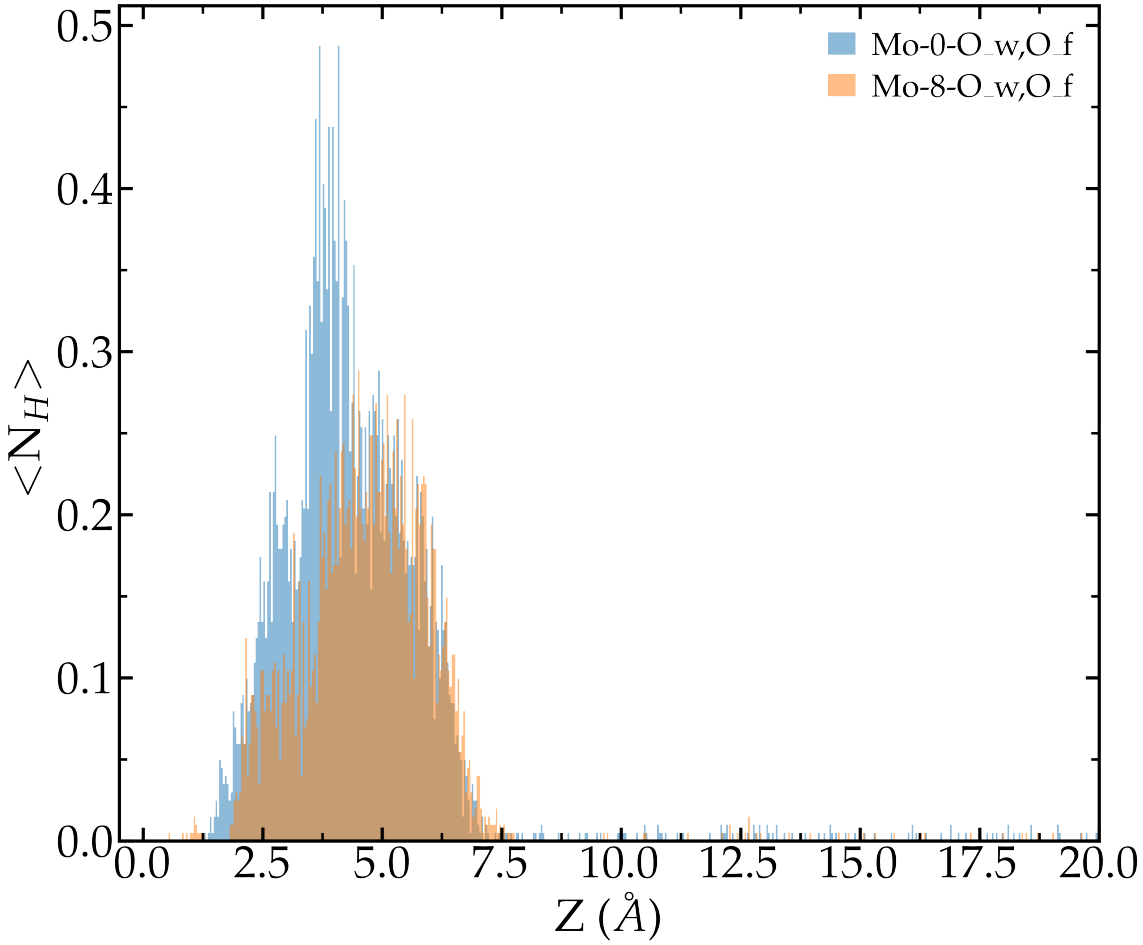

Figure 11: Effect of $[Mo]_{aq}$ on the HB abilities of water and Fh. Average number of hydrogen bonds as a function of distance from the surface for water oxygen O_w donors and surface oxygen O_f acceptors

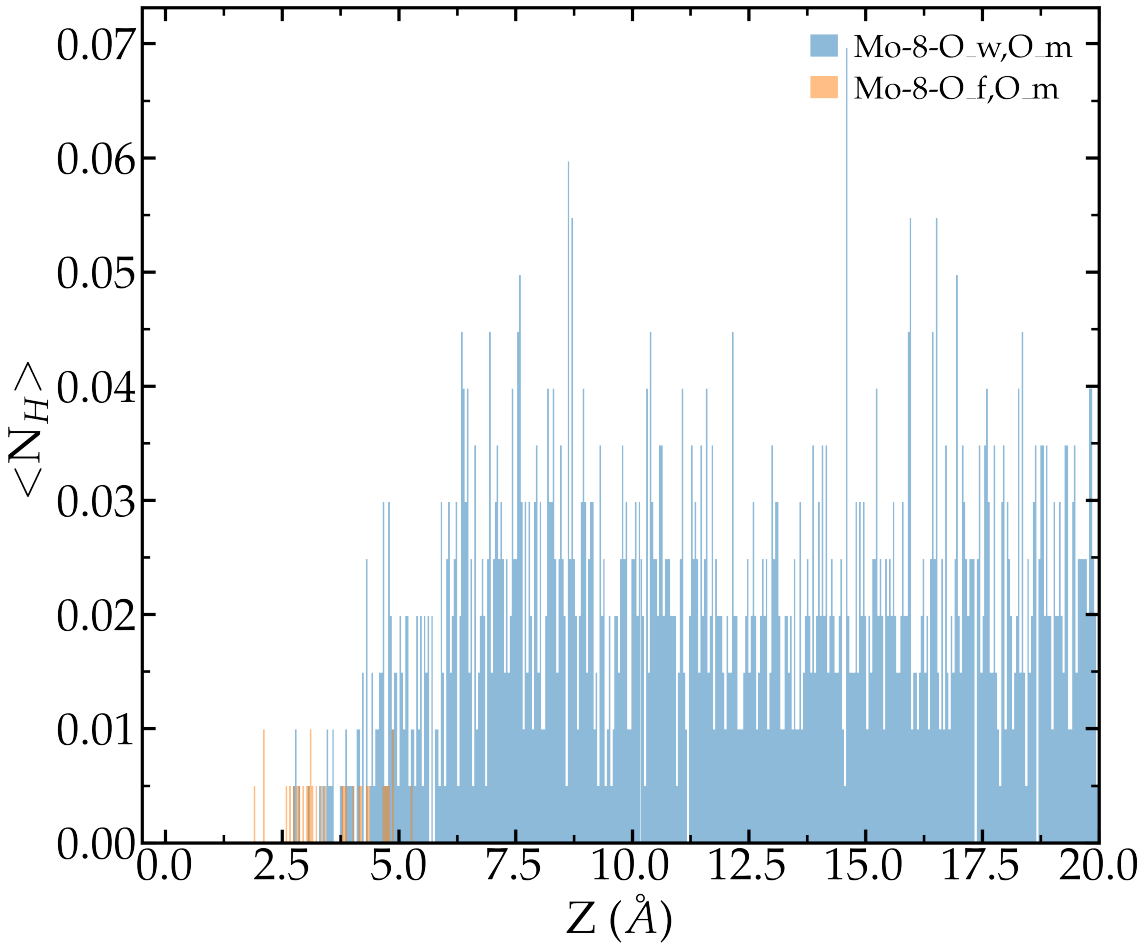

Figure 12: Effect of $[Mo]_{aq}$ on the HB abilities Mo_{aq}. Average number of hydrogen bonds as a function of distance from the surface for Mo_{aq} oxygen O_m acceptors and water oxygen O_w and surface oxygen O_f donors in Mo-8

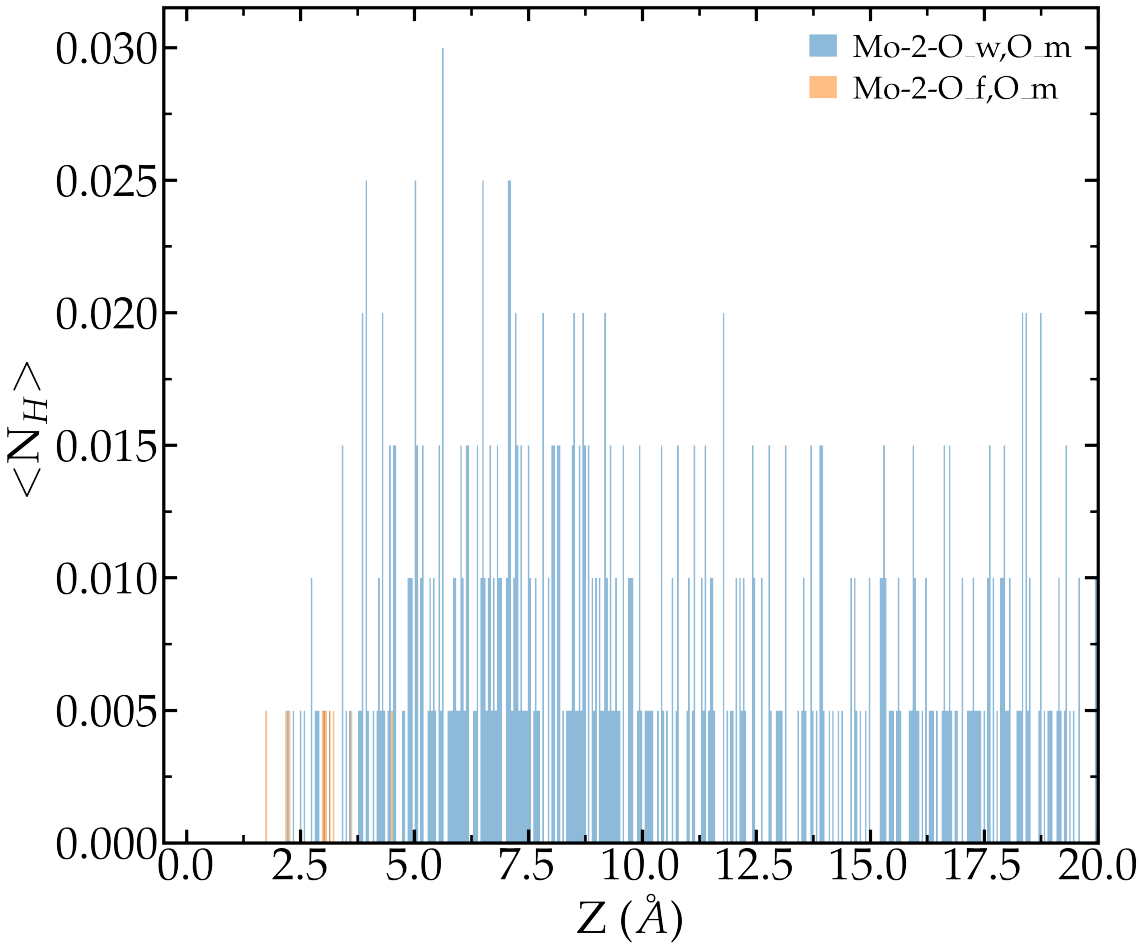

Figure 13: Effect of $[Mo]_{aq}$ on the HB abilities Mo_{aq}. Average number of hydrogen bonds as a function of distance from the surface for Mo_{aq} oxygen O_m acceptors and water oxygen O_w and surface oxygen O_f donors in Mo-2

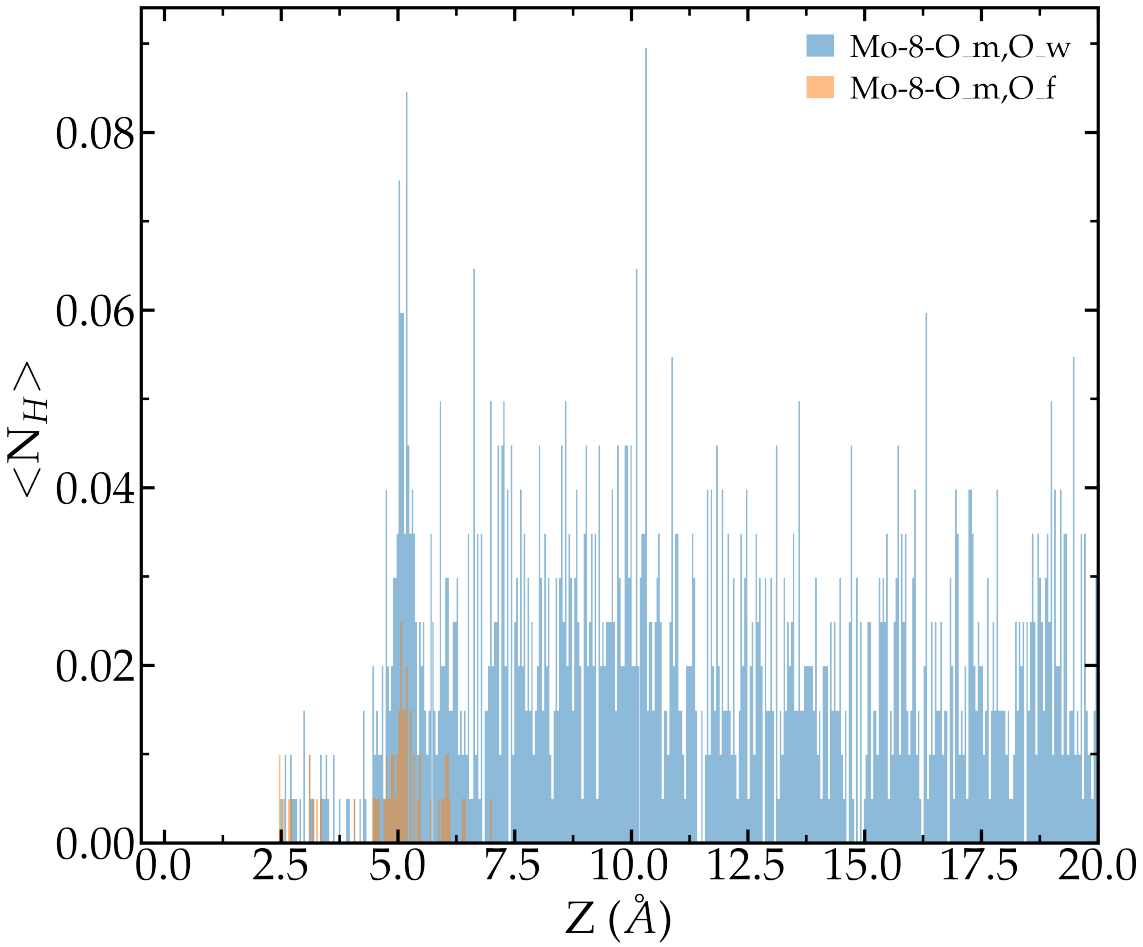

Figure 14: Effect of $[Mo]_{aq}$ on the HB abilities Mo_{aq}. Average number of hydrogen bonds as a function of distance from the surface for Mo_{aq} oxygen O_m donors and water oxygen O_w and surface oxygen O_f acceptors in Mo-8

7 Temporal Analysis of Intramolecular Distances

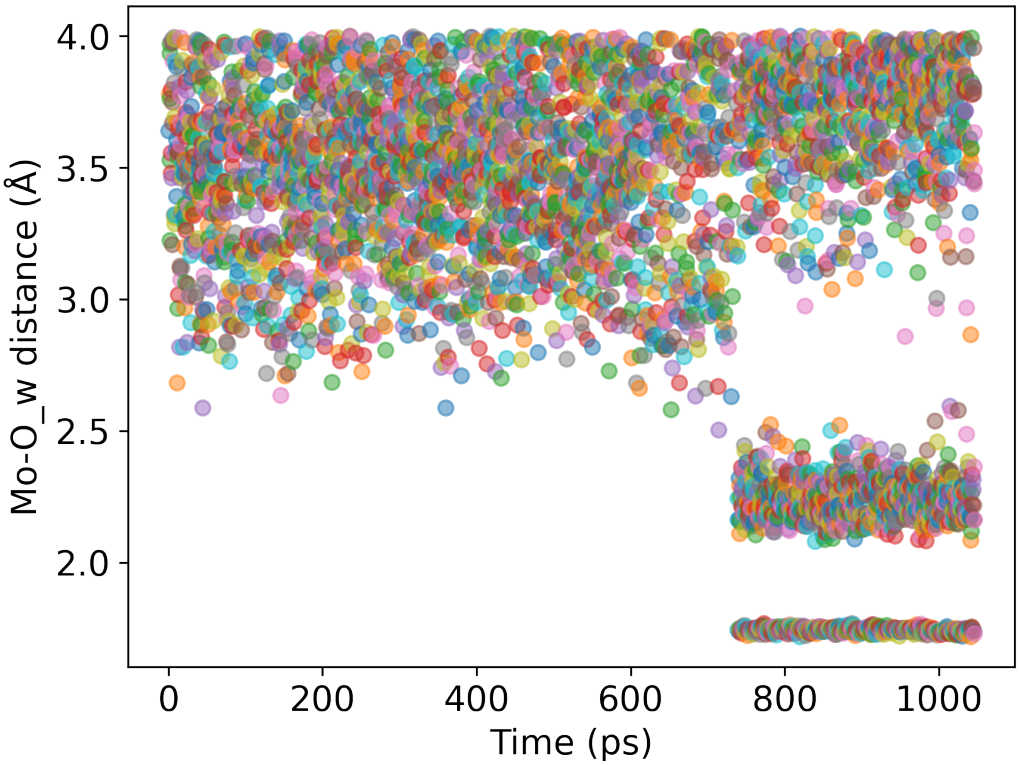

Figure 15: Monitoring the distances between Mo and water oxygens O_w in time. The distance profile for Mo_{aq} and water oxygen (O_w) in time.

8 Radial Distribution Function Analysis of Bulk Species

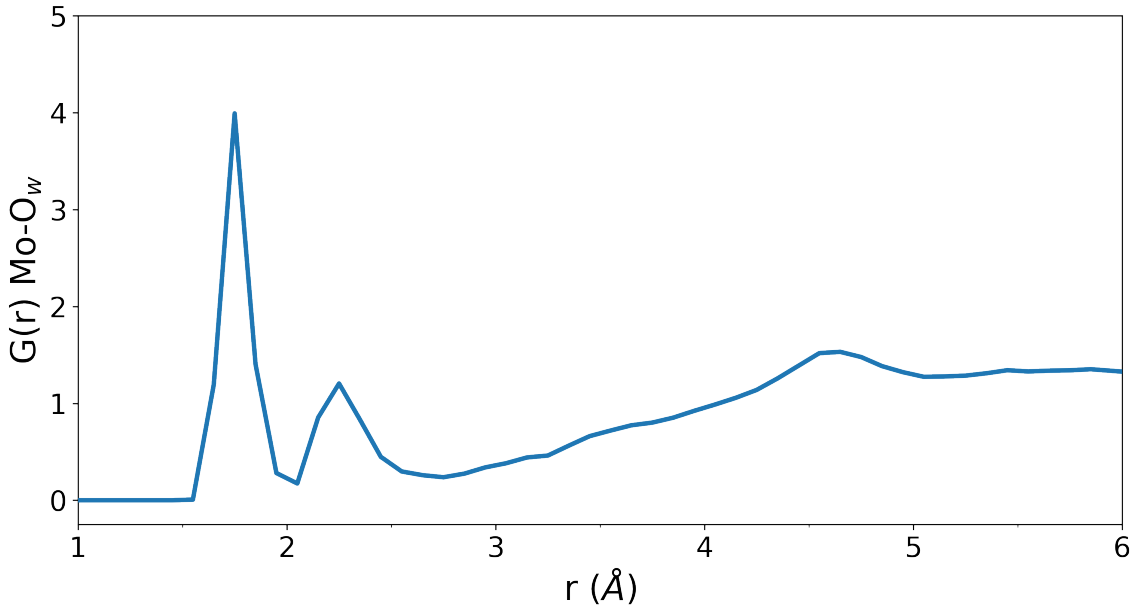

Figure 16: RDF of Mo_{aq} and water. RDF of Mo-Ow

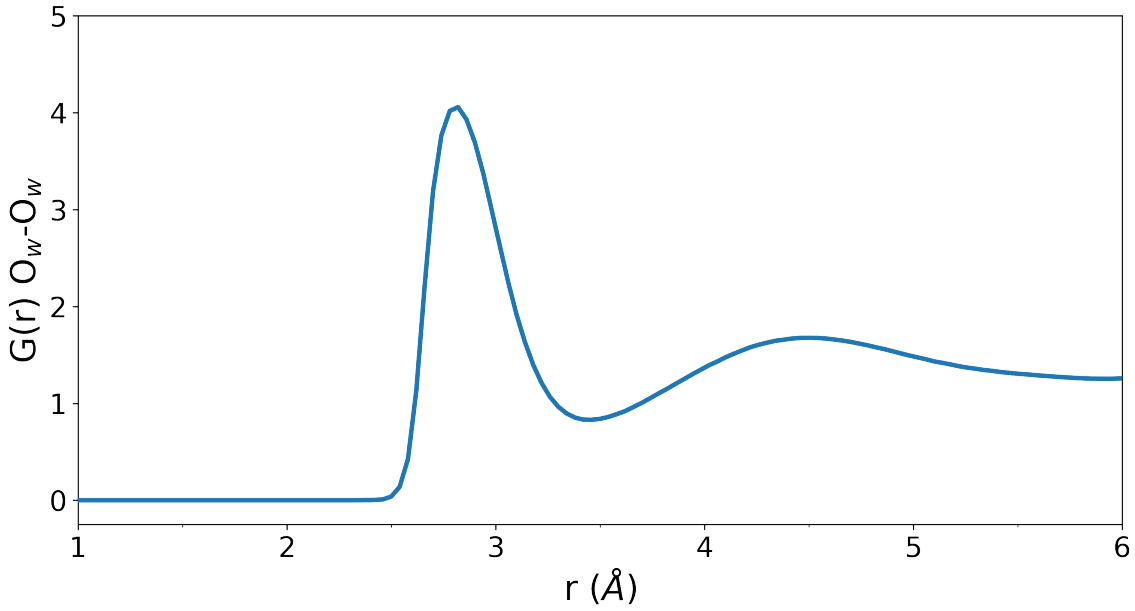

Figure 17: RDF of water. RDF of water O_w–O_w.

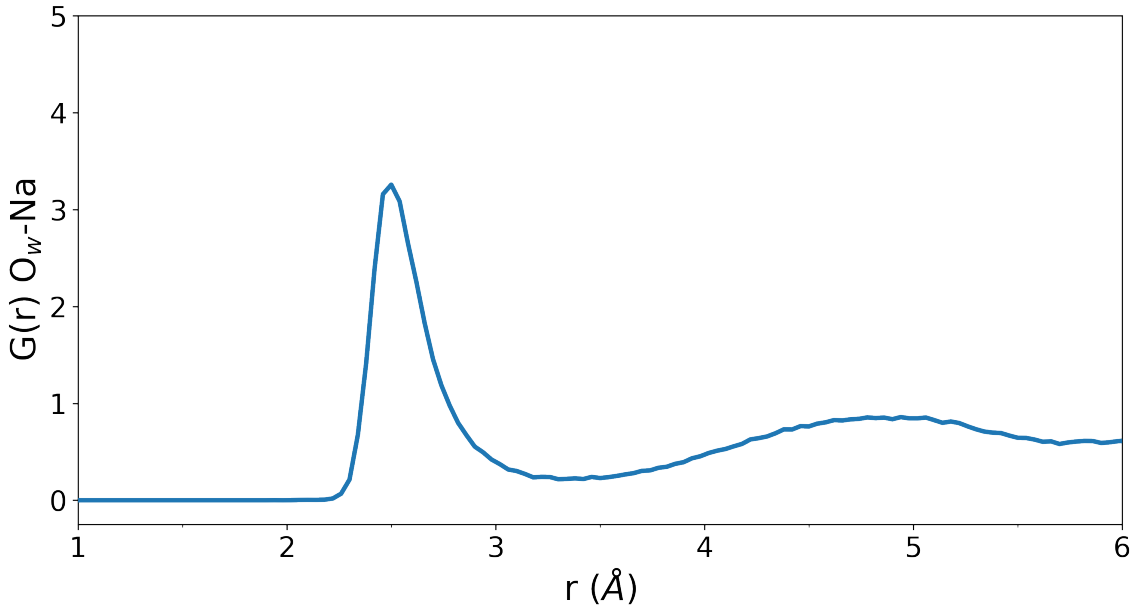

Figure 18: RDF of Na and water. RDF of Na and water oxygen Na–O_w

9 Electron Density Profile of Mo_{aq}

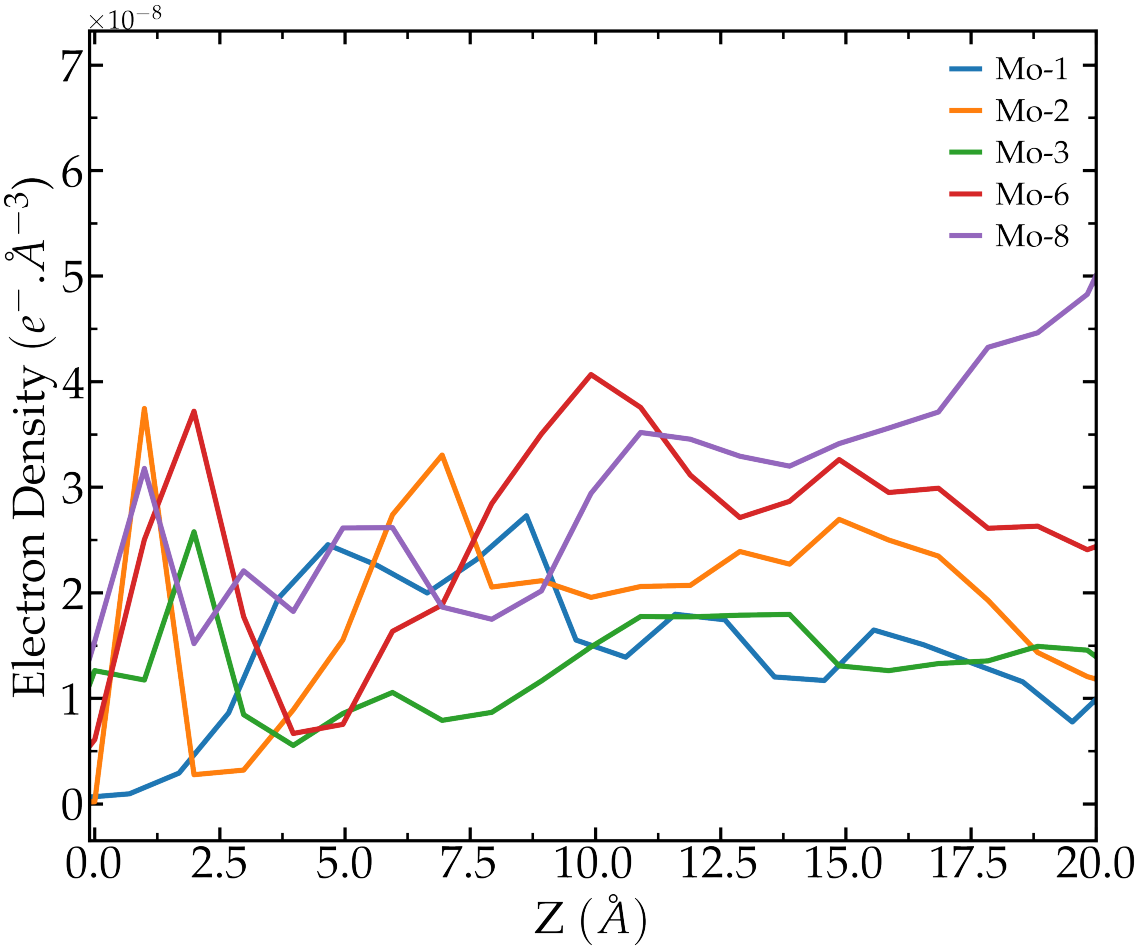

Figure 19: Electron density profile of Mo_{aq} at Fh-water interface. Stacked electron density profile of Mo_{aq} as a function of distance from the surface. The surface is defined as the top-most layer of Fh using ITIM algorithm.

10 Umbrella Sampling

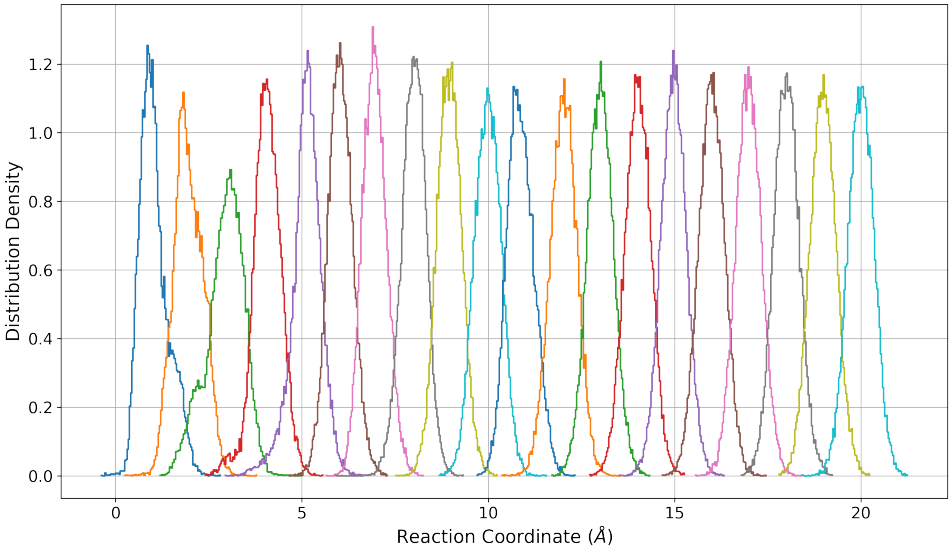

Figure 20: Umbrella Sampling Window Setup. Distribution density of distance from the surface collective variable within each umbrella sampling window for Mo-1

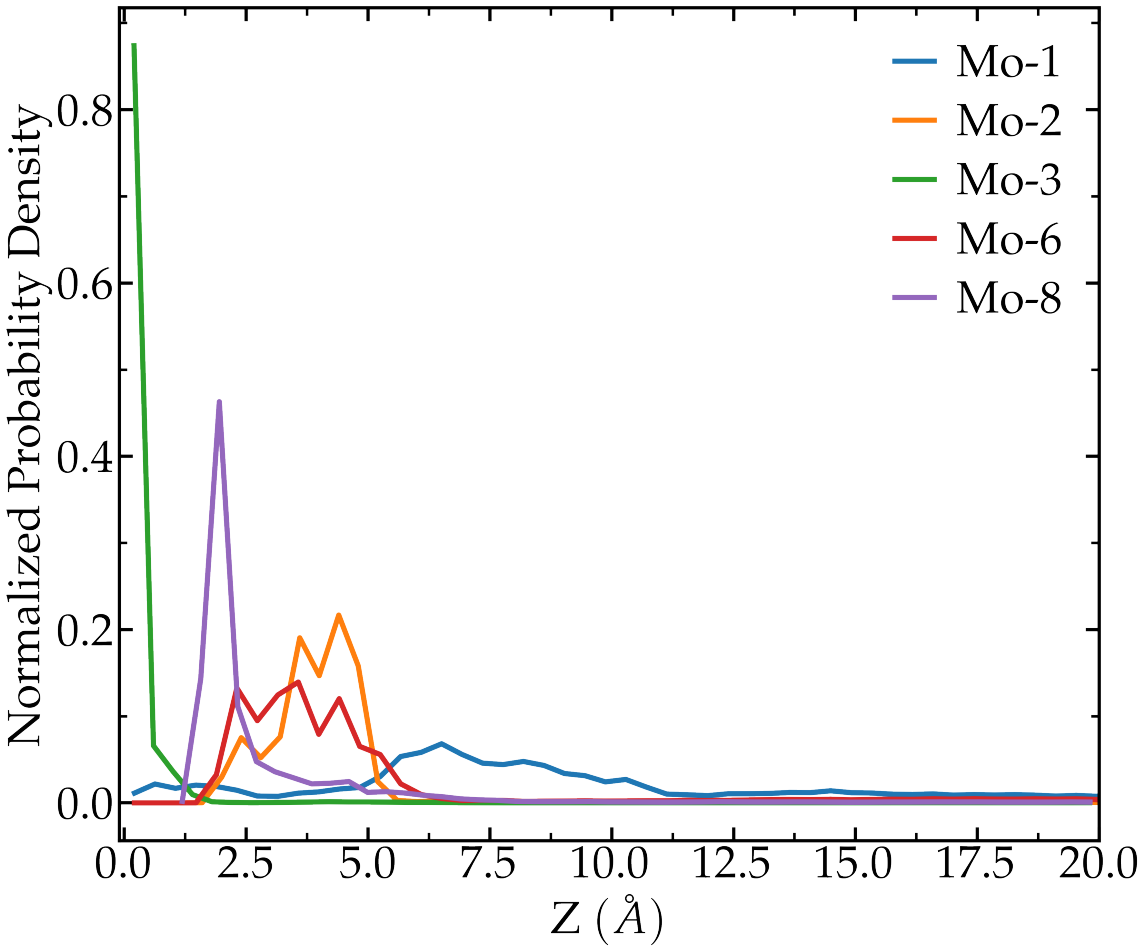

Figure 21: Probability analysis of Mo_{aq} from the surface by umbrella sampling. Normalized probability of Mo_{aq} as a function of distance from the surface of Fh.

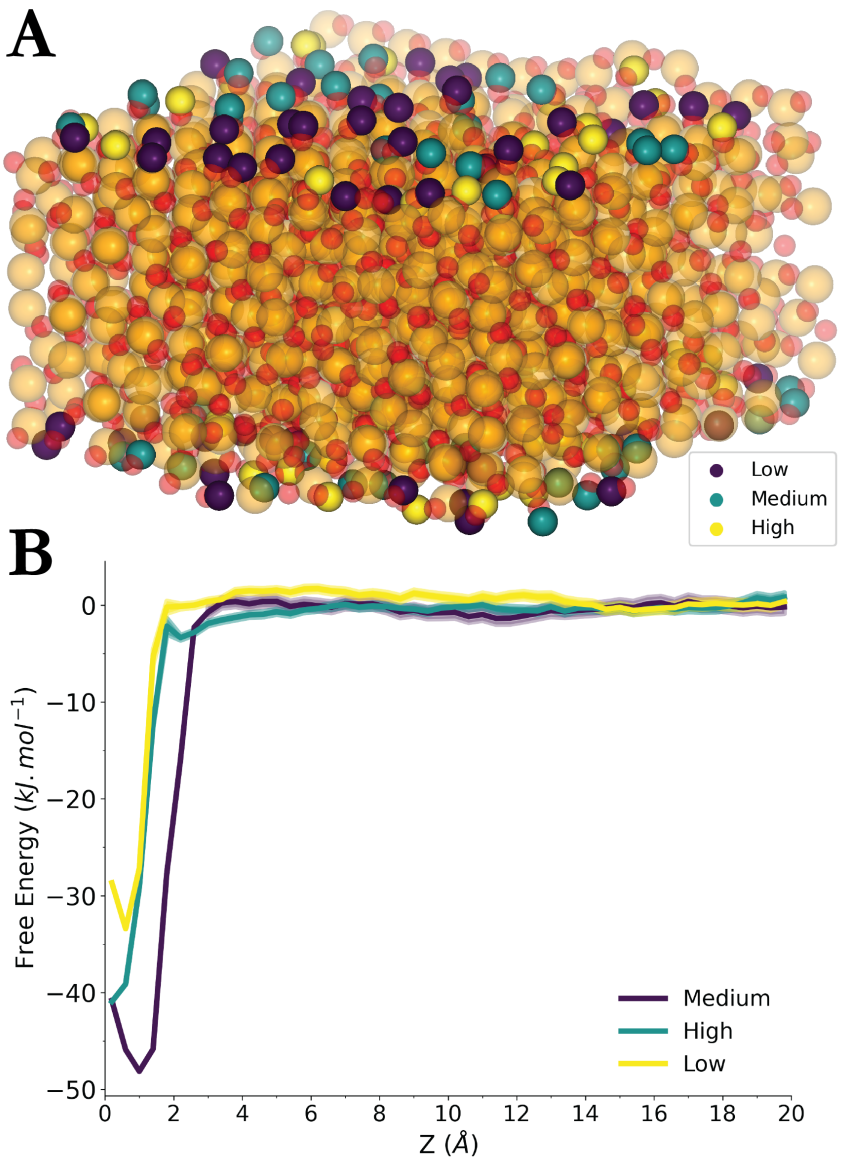

Figure 22: Acidity calculations of Fh surface protons via umbrella sampling. A) Fh surface protons at equilibrium, categorized based on their charge distributions into three percentiles of Low, Medium, and High charge. Red and orange spheres represent O and Fe atoms, respectively. B) Free energy profile of the surface deprotonation. Calculated free energies ΔG are based on the difference between the free energy of the proton at the bulk (>15 Å) and the lowest free Energy in profile representing the most stable state of the proton.

11 Ferrihydrite Slab Setup for Simulations

11.1 Bond Valence Sum

Dangling surface oxygens were protonated by hydrogen atoms based on the Bond Valence Sum (BVS) value derived K_H [2]. BVS is calculated using the following equation:

$$valence(O_i) = \sum_{n=0}^{i} e^{(\frac{1.759-R}{0.37})} \tag{1}$$

- R: Fe–O bond length (Å).

$LogK_H$ and pH=7 determine the protonation state of surface oxygens, calculated using BVS values and the following formula [2]:

$$LogK_H = -19.8(-2 + (mS_H) + (n \times (1 - S_H)) + valence(O_i)) \tag{2}$$

- m: Number of donating H bonds.
- n: Number of accepting H bonds.
- S_H = Valence of a H bonded to a surface oxygen (0.8)

Figure 23 shows the results of calculations resulting in mono-protonation for singly and doubly-coordinated surface oxygens (–OH and μ–OH), consistent with the infrared spectroscopy study of Fh [3].

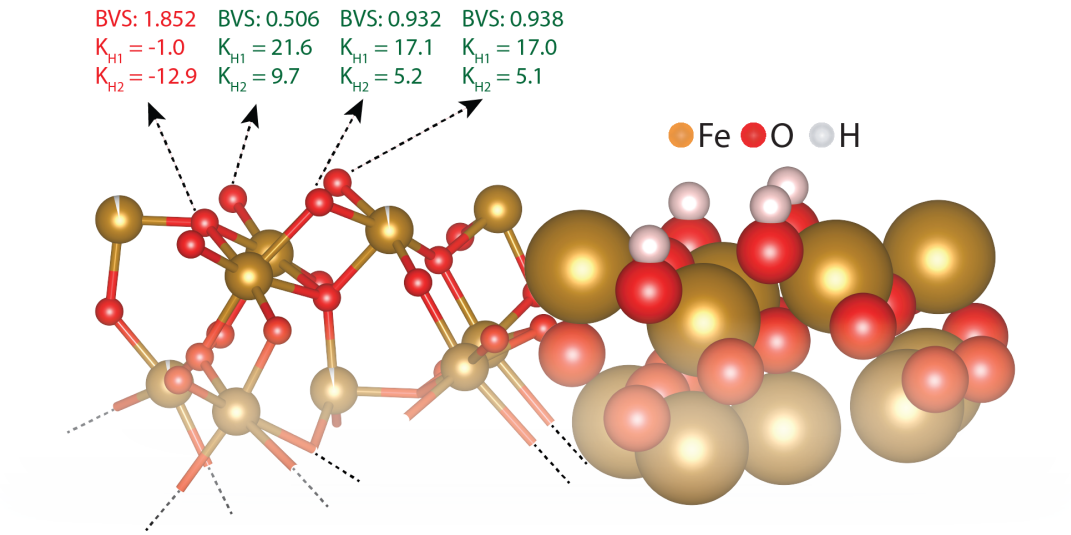

Figure 23: BVS analysis to determine the protonation state of Fh surface oxygens. Left: LogK_{H1}, LogK_{H2} and protonation state of surface oxygens of Fh determined by equation (2). Right: Protonated surface oxygens based on the working pH=7.

12 Simulation Details

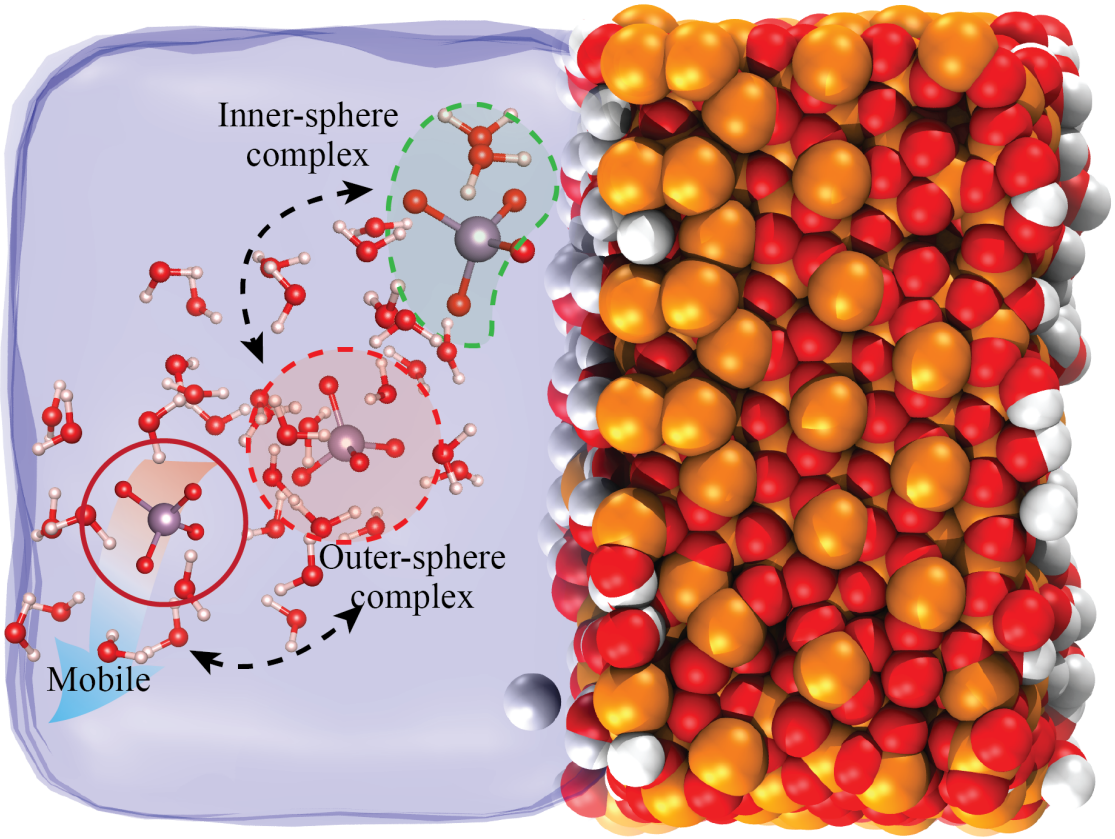

Figure 24: States of $[Mo]_{aq}$ in bulk water and at water-ferrihydite interface. Snapshot of the MD simulation with Mo in purple, O in red, H in white, and Fe in orange. Some water molecules are displayed as a transparent field for clarity. The dashed arrows show the exchanges between the three possible states for aqueous Mo: partially-solvated inner-sphere complexes (green shaded area), solvated outer-sphere complexes (red shaded area), and bulk. The colored arrow on the left highlights the fact that adsorption onto the surface of Fh determines the mobility and thus the fate of aqueous Mo.

Density profiles are calculated using the MAICoS toolkit (https://www.maicos-analysis.org). Identification of Truly Interfacial Molecules (ITIM) algorithm implemented in Pytim package was used to identify interfacial atoms/layers [4].

12.0.1 Definition of Surface

Unlike classical systems where explicit bonds or angles can be defined and referencing surface is possible by finding an average plane through a static set of atoms, in reactive MD the exchange of atoms, especially at the interface, allows the simulation of a *rough* surface further making finding where the surface ends challenging. ITIM algorithm allows overcoming this challenge by finding the interfacial atoms in each frame of the trajectory. The interfacial *Atomgroups* can be used for calculating correlation functions, charge density, and referencing the surface for (electron) density profiles. Figures 25, 26, and 27, show the interfacial layers of water and Fh determined by ITIM algorithm.

13 Error Analysis for Adsorption Constants

Calculated equilibrium constants were averaged using the weighing method explained by Dzombak *et. al.* [5] and the following equation:

Where w_i is the weight for each trajectory i and is calculated as using the uncertainty in $LogK_{a,i}$ denoted as σ_i:

$$w_i = \frac{\frac{1}{\sigma_i}}{\sum_{i=1}^{n} \frac{1}{\sigma_i}} \quad \text{for } i = \text{Mo-1}, \ldots, \text{Mo-8} \tag{3}$$

The weight-average $LogK_a$ is then calculated by:

$$\text{Weighted } LogK_a = \frac{\sum_{i=1}^{n} w_i \times LogK_{a,i}}{\sum_{i=1}^{n} w_i} \quad \text{for } i = \text{Mo-1}, \ldots, \text{Mo-8} \tag{4}$$

14 Identification of Truly Interfacial Molecules Analysis

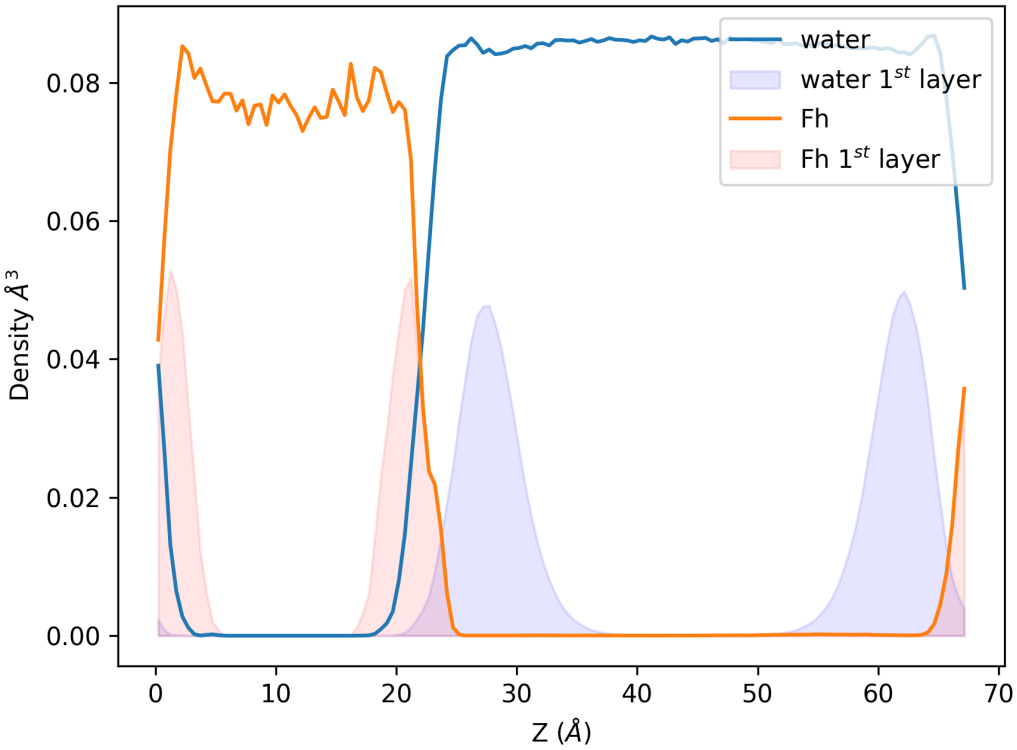

Figure 25: ITIM analysis of Fh-water interface. Density profiles of Fh and water and their respective interfacial layers in Mo-1.

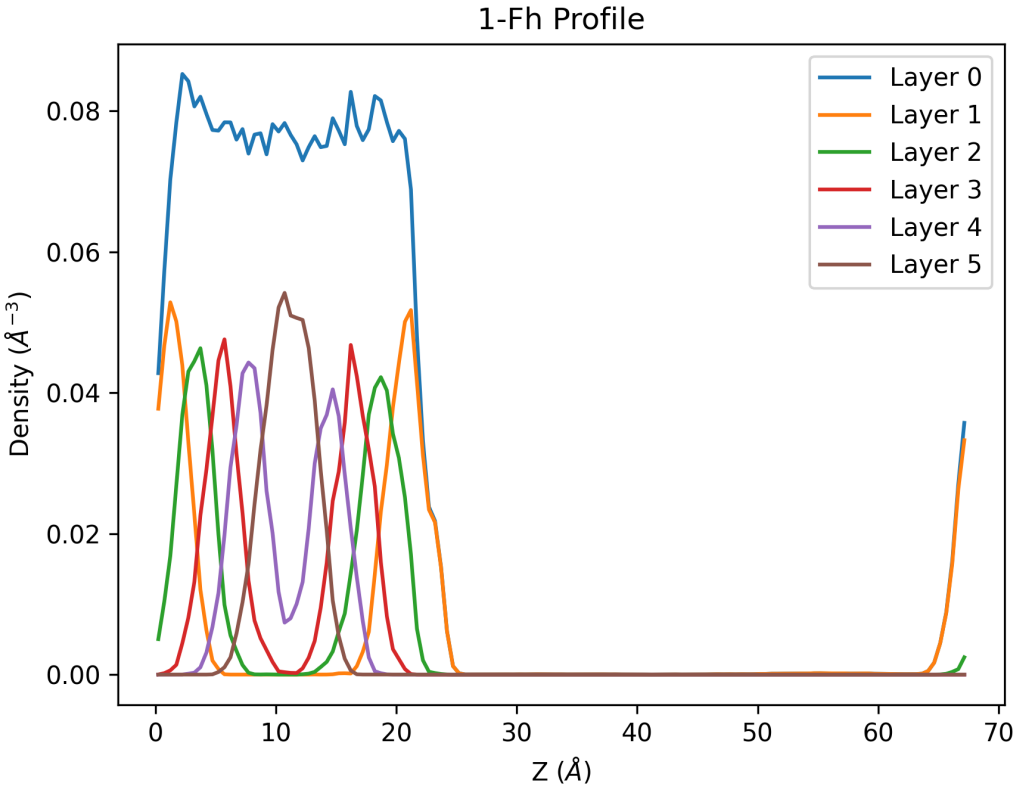

Figure 26: ITIM analysis of Fh-water interface: Fh layers. Density profile of Fh and its consisting layers in Mo-1.

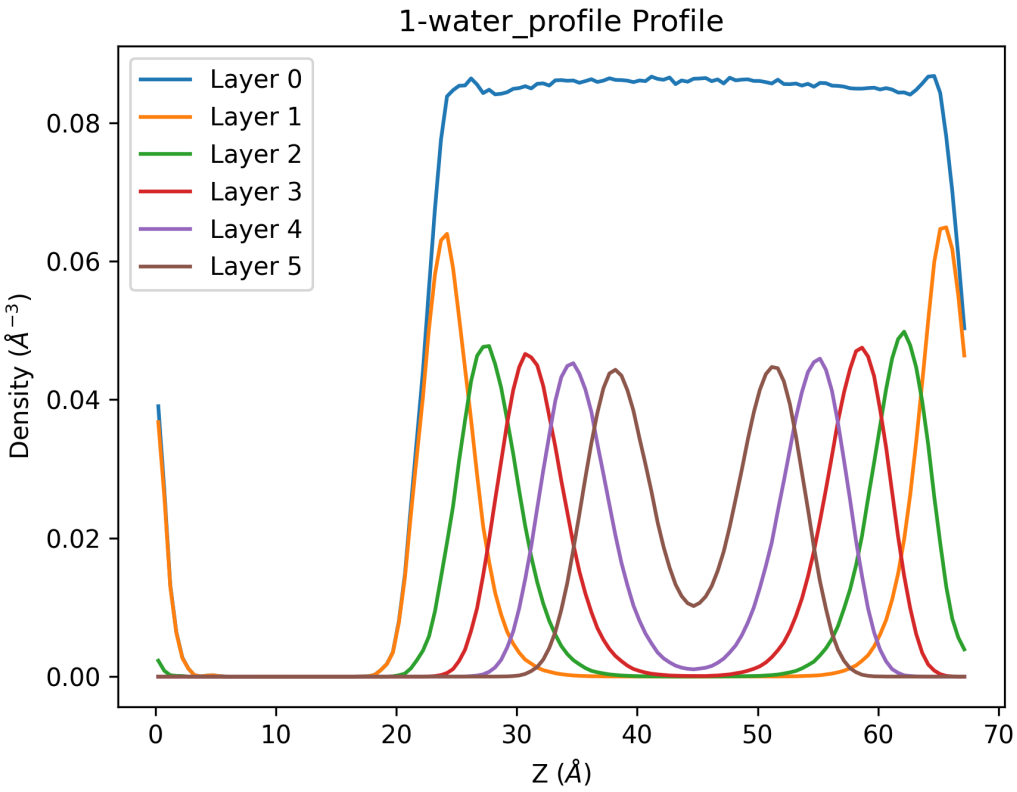

Figure 27: ITIM analysis of Fh-water interface: water layers. Density profile of water and its consisting layers in Mo-1.

References

[1] Richard Gowers, Max Linke, Jonathan Barnoud, Tyler Reddy, Manuel Melo, Sean Seyler, Jan Domański, David Dotson, Sébastien Buchoux, Ian Kenney, and Oliver Beckstein. MDAnalysis: A python package for the rapid analysis of molecular dynamics simulations. In *Proceedings of the Python in Science Conference*. SciPy, 2016.

[2] Peter Venema. *Charging and ion adsorption behaviour of different iron (hydr) oxides*. Venema, 1997.

[3] Jean-François Boily and Xiaowei Song. Direct identification of reaction sites on ferrihydrite. *Communications Chemistry*, 3(1), June 2020.

[4] Marcello Sega, György Hantal, Balázs Fábián, and Pál Jedlovszky. Pytim: A python package for the interfacial analysis of molecular simulations. *Journal of Computational Chemistry*, 39(25):2118–2125, sep 2018.

[5] David A Dzombak and Francois MM Morel. *Surface complexation modeling: hydrous ferric oxide*. John Wiley & Sons, 1991.